

Effects of Dielectric Particles on Non-Oxidative Coupling of Methane in a Dielectric Barrier Discharge Plasma Reactor

*Juchan Kim¹, Jaekwon Jeoung¹, Jonghyun Jeon¹, Jip Kim¹, Young Sun Mok², Kyoung-Su
Ha^{*,1}*

¹ Department of Chemical and Biomolecular Engineering, Sogang University, 35 Baekbeom-ro, Mapo-gu, Seoul 04107, Republic of Korea

² Department of Chemical and Biological Engineering, Jeju National University, Jeju, 63243, Republic of Korea

Corresponding Author

*To whom all correspondence should be addressed. Tel.: (+82)-2-3274-4892, Fax: (+82)-2-711-0439, E-mail: philoseus@sogang.ac.kr

List of Contents

Table S1. The molar balances on hydrogen and carbon in each test.

Table S2. Various non-oxidative methane coupling reaction performances in a DBD plasma reactor.

Table S3. Maximum experimental errors in packed bed tests with various packing materials

Table S4. Physisorption result of each sample.

Figure S1. Schematic diagram of packed bed DBD plasma system.

Figure S2. N₂ physisorption results; (a) Isotherms (b) BJH pore size distribution curves of the fresh KIT-6 samples.

Figure S3. Small-angle X-ray scattering patterns of (a-b) fresh & spent KIT-6 (S), (c-d) fresh & spent KIT-6 (M), and (e-f) fresh & spent KIT-6 (L).

Figure S4. Q-V Lissajous plots of (a) α -Al₂O₃ samples, (b) sea sand samples, and (c) KIT-6 samples. (S), (M), and (L) denote the size of each sample.

Figure S5 Voltage-current profiles in the blank DBD reactor.

Figure S6. Reaction performances when no particles (blank), α -Al₂O₃, sea sand, and KIT-6 were used at TOS 380 min; (a) CH₄ conversion and product selectivity (b) CH₄ conversion and product yield.

Figure S7. SEM image of (a) spent α -Al₂O₃ (S), (b) spent α -Al₂O₃ (M), (c) spent α -Al₂O₃ (L), (d) spent sea sand (S), (e) spent sea sand. (M), (f) spent sea sand (L), (g) spent KIT-6 (S), (h) spent KIT-6 (M), and (i) spent KIT-6 (L).

Figure S8. TEM imaging analyses with EDS of (a) spent α -Al₂O₃, (b) spent sea sand, and (c) spent KIT-6.

Table S1

The molar balances on hydrogen and carbon in each test.

Sample	Blank	α -Al ₂ O ₃			sea sand			KIT-6		
Size	-	S	M	L	S	M	L	S	M	L
TOS 60 min										
CB (%) ^a	94.22	98.18	82.70	86.68	79.97	75.02	81.10	96.84	75.86	85.72
HB (%) ^b	97.01	98.57	93.51	93.65	95.46	95.09	92.41	99.77	92.03	94.47
TOS 300 min										
CB (%) ^a	93.50	94.00	95.44	95.89	99.12	98.09	90.61	98.71	97.49	94.12
HB (%) ^b	96.09	93.33	95.11	97.19	100.00	99.79	97.43	99.06	98.77	97.14

$$^a \text{ Carbon Balance (CB) (\%)} = \frac{\text{Moles of CH}_4 \text{ not converted} + \sum(x \times \text{Moles of C}_x\text{H}_y \text{ produced})}{\text{Moles of CH}_4 \text{ in the feed}} \times 100$$

$$^b \text{ Hydrogen Balance (HB) (\%)} = \frac{4 \times \text{Moles of CH}_4 \text{ not converted} + 2 \times \text{Moles of H}_2 \text{ produced} + \sum(y \times \text{Moles of C}_x\text{H}_y \text{ produced})}{4 \times \text{Moles of CH}_4 \text{ in the feed}} \times 100$$

Table S2

Various non-oxidative methane coupling reaction performances in a DBD plasma reactor.

Temperature / re / Pressure	Feed	Packing material	Voltage/Fr equency/Power	CH ₄ conversion (%)	Product selectivity (%)				Referenc e	
					C ₂ H ₂	C ₂ H ₄	C ₂ H ₆	C ₃		C ₄
25 °C / 1 atm	40 sccm of CH ₄ /N ₂ = 1	SiO ₂ , Al ₂ O ₃	15 kV / 1 kHz / 36.1 – 44.1 W	19.9 – 58.4	11.2 – 46.5	4.70 – 12.7	9.56 – 21.8	6.43 – 10.7	3.86– 25.2	This study
20 °C / 1 atm	30 sccm of 90 % CH ₄ , 10 % Ar	Blank	7.2 kV / 2 kHz / 9.6 W	9.7	Not included	3.3	24.6	8.3	2.6	
Not included	200 sccm of 10 % CH ₄ , 90 % Ar	MgO/Al ₂ O ₃	6 kV / 3 kHz / 3.2 – 3.5 W	9.5 – 23	10.5 - 28	18.6 – 30.3	27.4 – 48.1	8.7 – 23.7	0.3 – 0.7	[2]
25 °C / 1 atm	30 sccm of 100 % CH ₄	Blank	20 kV / 60 W	13.8	1.23	3.26	14.8	6.74	5	[3]

Table S3

Maximum experimental errors in packed bed tests with various packing materials

Packing	Maximum error (%) ^a						
material	CH₄ conv.	C₂H₂ sel.	C₂H₄ sel.	C₂H₆ sel.	C₂ HC sel.	C₃ HC sel.	C₄ HC sel.
KIT-6	0.15	5.69	2.43	11.92	5.59	8.45	4.25
α-Al₂O₃	1.22	7.67	6.87	1.90	6.31	3.19	0.86
γ-Al₂O₃	0.17	10.35	12.00	3.16	8.58	5.17	3.33

^a Maximum error (%) = $\max \left(\left| \frac{\text{experimental value} - \text{mean experimental value}}{\text{mean experimental value}} \right| \right) \times 100$ (%)

Table S4

Physisorption result of each sample.

Sample	BET Surface Area (m ² /g)
α -Al ₂ O ₃ (S)	22.8
α -Al ₂ O ₃ (M)	18.0
α -Al ₂ O ₃ (L)	12.9
sea sand (S)	n.d.
sea sand (M)	n.d.
sea sand (L)	n.d.
KIT-6 (S)	898
KIT-6 (M)	892
KIT-6 (L)	777

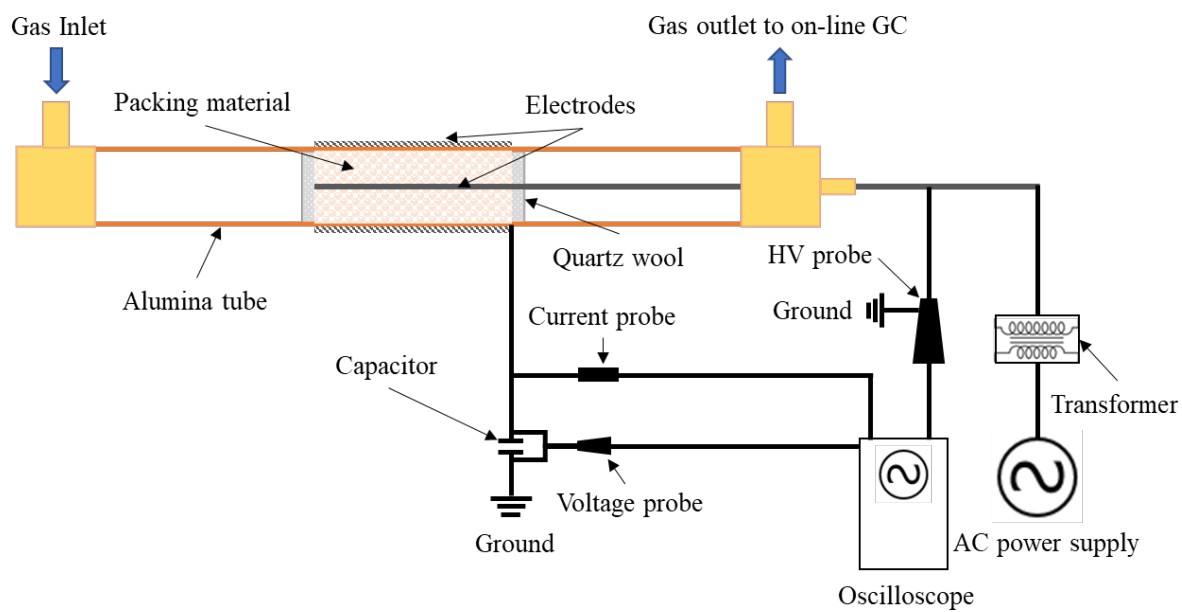


Figure S1. Schematic diagram of packed bed DBD plasma system.

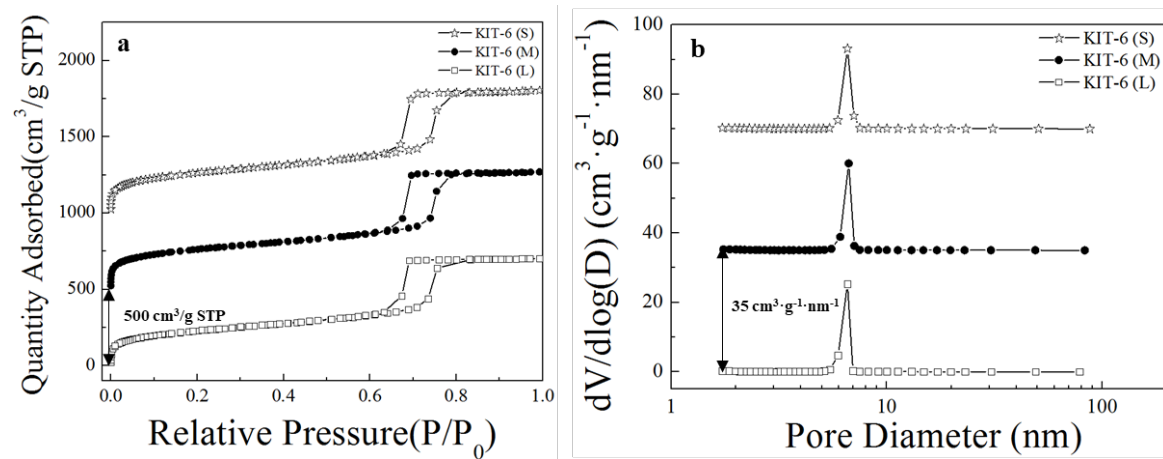


Figure S2. N₂ physisorption results; (a) Isotherms (b) BJH pore size distribution curves of the fresh KIT-6 samples.

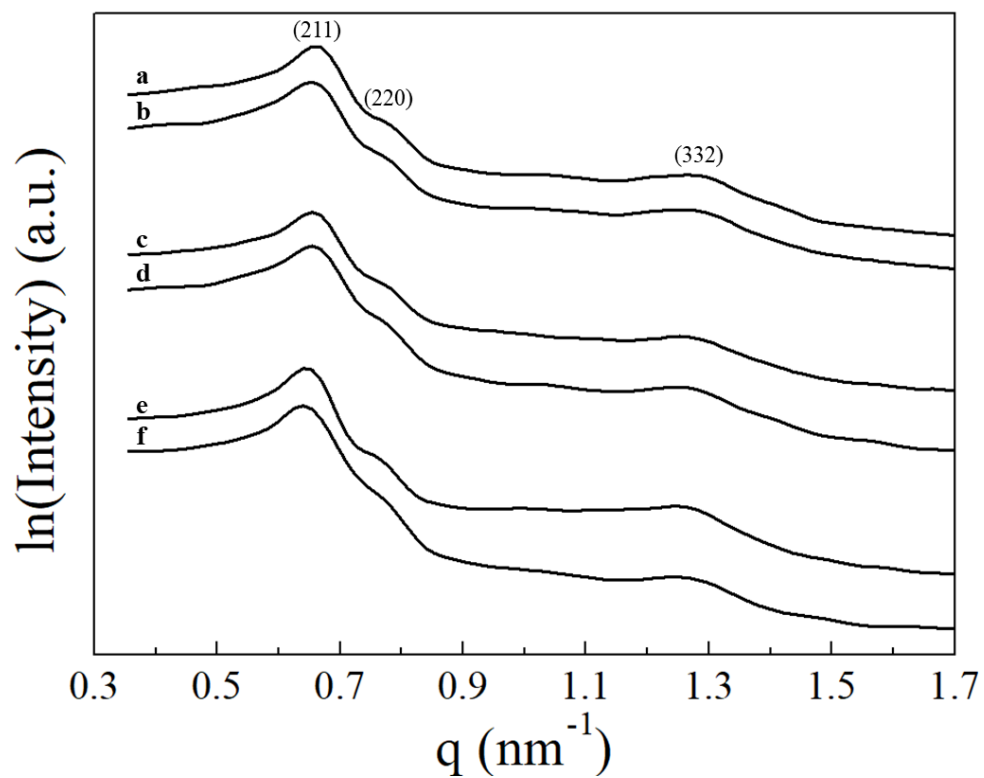


Figure S3. Small-angle X-ray scattering patterns of (a-b) fresh & spent KIT-6 (S), (c-d) fresh & spent KIT-6 (M), and (e-f) fresh & spent KIT-6 (L).

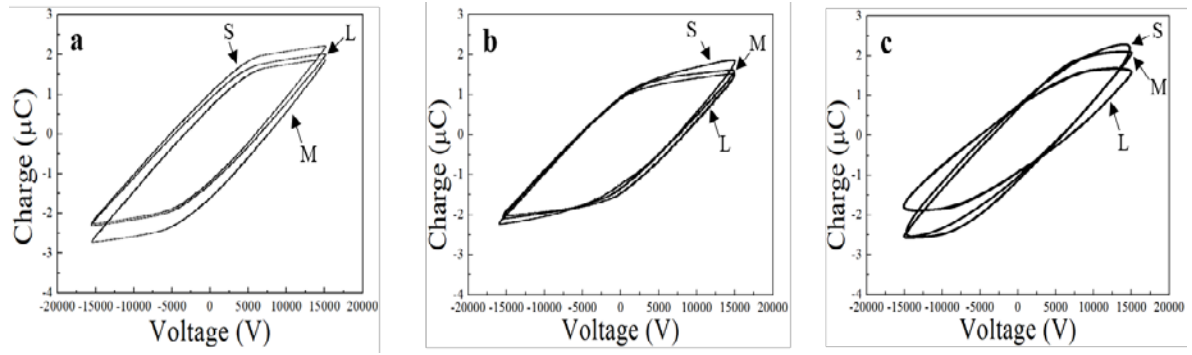


Figure S4. Q-V Lissajous plots of (a) α -Al₂O₃ samples, (b) sea sand samples, and (c) KIT-6 samples. (S), (M), and (L) denote the size of each sample.

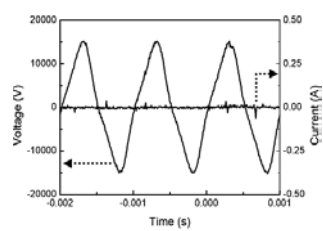


Figure S5. Voltage-current profiles in the blank DBD reactor.

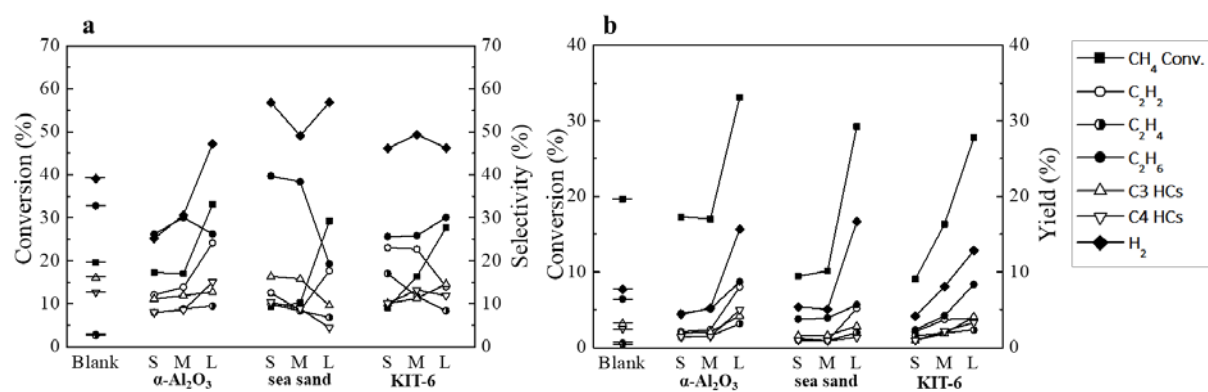


Figure S6. Reaction performances when no particles (blank), $\alpha\text{-Al}_2\text{O}_3$, sea sand, and KIT-6 were used at TOS 380 min; (a) CH₄ conversion and product selectivity (b) CH₄ conversion and product yield.

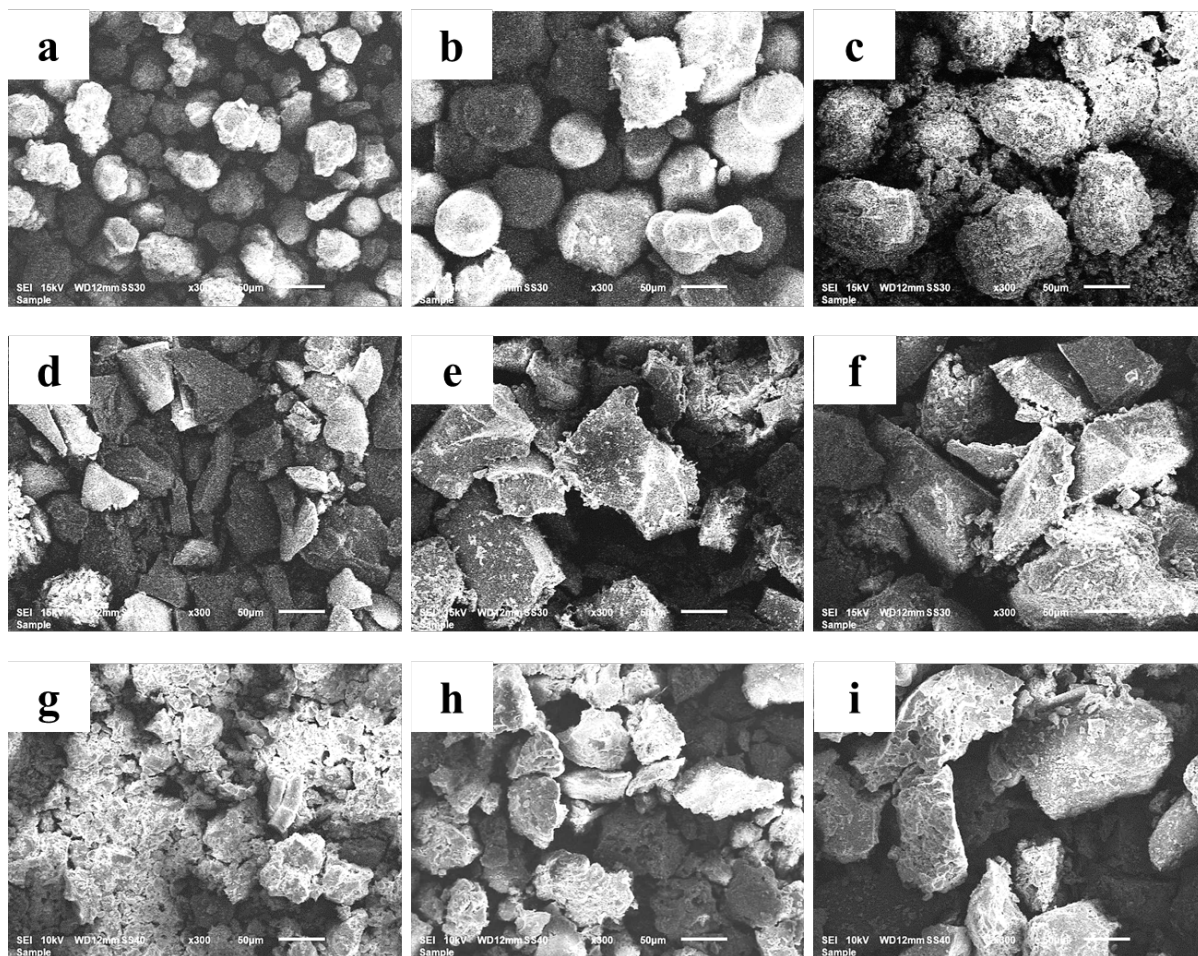


Figure S7. SEM image of (a) spent α -Al₂O₃ (S), (b) spent α -Al₂O₃ (M), (c) spent α -Al₂O₃ (L), (d) spent sea sand (S), (e) spent sea sand (M), (f) spent sea sand (L), (g) spent KIT-6 (S), (h) spent KIT-6 (M), and (i) spent KIT-6 (L).

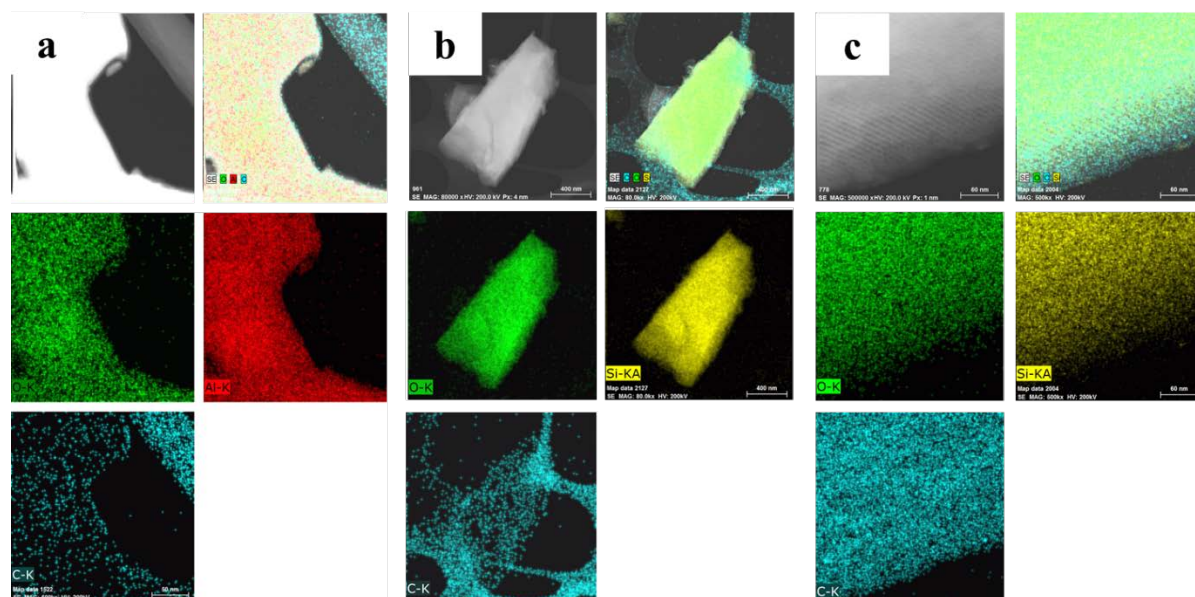


Figure S8. TEM imaging analyses with EDS of (a) spent α - Al_2O_3 , (b) spent sea sand, and (c) spent KIT-6.

References for Supplementary Information

- [1] S. Kudryashov, A. Ryabov, G. Shchyogoleva, A new approach to the non-oxidative conversion of gaseous alkanes in a barrier discharge and features of the reaction mechanism, *Journal of Physics D: Applied Physics* 49 (2015) 025205.
- [2] P. Kasinathan, S. Park, W.C. Choi, Y.K. Hwang, J.-S. Chang, Y.-K. Park, Plasma-Enhanced Methane Direct Conversion over Particle-Size Adjusted $\text{MO}_x/\text{Al}_2\text{O}_3$ (M= Ti and Mg) Catalysts, *Plasma Chemistry and Plasma Processing* 34 (2014) 1317-1330.
- [3] A. Indarto, N. Coowanitwong, J.-W. Choi, H. Lee, H.K. Song, Kinetic modeling of plasma methane conversion in a dielectric barrier discharge, *Fuel Processing Technology* 89 (2008) 214-219.